Characteristics of the precipitation concentration and their relationship with the precipitation structure: A case study in the Huai River basin, China

Yixing Yin [a,*], Haishan Chen [b], Guojie Wang [c], Wucheng Xu [d], Shenmin Wang [c], Wenjun Yu [a]

[a] School of Hydrology and Water Resources, Nanjing University of Information Science and Technology, Nanjing, Jiangsu 210044, China
[b] Key Laboratory of Meteorological Disaster of Ministry of Education, Nanjing University of Information Science and Technology, Nanjing, Jiangsu 210044, China
[c] School of Geographical Sciences, Nanjing University of Information Science and Technology, Nanjing 210044, China
[d] School of Land and Resources, China West Normal University, Nanchong 637002, China

A B S T R A C T

Concentrated heavy precipitation has a great potential to cause severe flood disasters, especially in densely populated areas. However, the influencing factors of the spatio-temporal changes of precipitation concentration have not been well understood and the relationship between the characteristics of precipitation concentration and the structure of precipitation has rarely been investigated so far. This study explored the concentration characteristics of precipitation based on the Gini coefficient and further investigated the relationship of the precipitation concentration with the precipitation structure by means of a set of precipitation indices based on the daily precipitation data from 1960 to 2014 in the climatic transition zone of the Huai River basin (HRB), China. Results show that: (1) There is a non-significant upward trend for the Gini in the HRB. The mean of the Gini coefficient shows a spatial pattern of increase from the south to the north, and the standard deviation (SD) of the Gini shows a pattern of increase from the northeast to the southwest. (2) The composite mean of the Gini in the drought years is larger than that in the flood years for all the stations. And the composite SD of the Gini in the flood years is larger than that in the drought years for most of the stations. (3) The non-significant increase of the Gini in the HRB is mainly associated with AR (Annual rainfall), RD (Rainy days), the light and moderate rainfall (mainly PF20, PF40, PF50) and the wet-day and dry-day indices (PPWW, PWSAV, PPDD and PDSAV).

1. Introduction

Floods and droughts are the major natural hazards which can threaten the agriculture, people and economic development in the world. However, large parts of the world are suffering from more serious floods and droughts under the background of climatic change (Jongman et al., 2012; Dai, 2013; Visser et al., 2014). The spatial and temporal variability of precipitation may lead to both floods and droughts. The characteristics of the precipitation have been changing both globally (Groisman et al., 2005) and regionally (Zhai et al., 2005; Simpson and Jones, 2014) under the influences of climatic change and anthropogenic activities. Therefore, it is crucial for the assessment of flood/drought risks and the water resources management to better understand the precipitation variability at various time scales over different areas.

With the acceleration of the water cycle under the background of greenhouse warming, rainfall tends to become more concentrated in many parts of the world (Li et al., 2017; Serrano-Notivoli et al., 2018).

Recently, the characteristics of precipitation concentration have attracted more and more attention. The precipitation concentration includes the degree that the precipitation concentrates in both space and time, but mainly refers to the temporal concentration. The characters of precipitation concentration have important implications for the understanding of floods and droughts. And concentrated heavy precipitation has a great potential to cause severe disasters, especially in densely populated areas (Nery et al., 2017).

The concentration of precipitation can be characterized by using several methods, and numerous studies have examined the spatial and temporal characters of the precipitation concentration with different indices. Martin-Vide (2004) defined a concentration index of the precipitation (abbreviated hereafter as CI) to assess the contribution of the days with extreme rainfall to the total rainfall. The second index which can be utilized to estimate the monthly precipitation irregularity in the year is the precipitation concentration index suggested firstly by Oliver (1980) (abbreviated hereafter as PCI). Zhang and Qian (2003) put

forward two kinds of indices to assess the concentration characters of the precipitation, one is the precipitation concentration degree (PCD) and the other is the precipitation concentration period (PCP). The third concentration measure of dimensionless index which is frequently used is the Gini coefficient (Rajah et al., 2014).

A large number of researches have revealed the characters and the spatio-temporal changes of the precipitation concentration around the world (Rajah et al., 2014; Yesilirmak and Atatanir, 2016; Zubieta et al., 2017; Royéa and Martin-Videb, 2017; Llano, 2018). However, to the best of our knowledge, the influencing factors and mechanisms of the changes of the precipitation concentration have not been well understood so far, especially under the changing environment of intensified anthropogenic activities and global warming. And this issue has also attracted many researchers' attention. Royéa and Martin-Videb (2017) found that there were linear relationships between the CI and some geographical elements such as latitude, longitude and altitude. Huang et al. (2018), Sarricolea et al. (2019) also investigated the correlations between the precipitation concentration indices (PCI, PCD, PCP and CI) and the geographic elements including latitude, longitude and elevation. Benhamrouche et al. (2015) correlated the CI index with some other precipitation parameters, such as the annual total precipitation, the number of rainy days and the annual variation coefficient. Jiang et al. (2016) examined whether there existed links between precipitation concentration and the urbanization, and obtained significant positive correlation in three selected regions. Zheng et al. (2017) examined the link between elevation and precipitation concentration and tried to identify the contributions of the influencing factors based on seven large-scale climatic indices in the Pearl River basin. Most recently, Rahman and Islam (2019) explored the changes of precipitation concentration and intensity and the possible causes of changes in precipitation systems in Bangladesh; Guo et al. (2020) tried to explore the potential influence of precipitation concentration on drought; Yang et al. (2020) proved that the change in precipitation concentration had closely relationship with some teleconnection indices in central Asia.

The eastern part of China belongs to a monsoon climate, and the monsoon climate is usually characterized as high intensity of the rainfall in the rainy season, and thus the precipitation concentration is very high in eastern China. The Huai River basin (HRB) is situated in the transitional belt of the north and south of China. The Huai River is one of the biggest seven rivers in China and the HRB is also one of the most densely inhabited basins, one of the most important economic zones and agricultural centers in China. The precipitation concentration in this region is very high, causing serious flood and drought disasters. At present, serious water problems are prevalent in the HRB, such as flood and drought disasters, water shortages, high reservoir-induced hydrological regulation, serious water pollution and aquatic ecological degradation (Zhang et al., 2010; Zhao et al., 2014).

The eastern Asian summer monsoon (EASM) is one of the main factors which determining the precipitation in the HRB. Yin et al. (2019) investigated the relationship between summer extreme precipitation and EASM in the HRB. Zheng et al. (2017) indicated that EASM is the most significant factor affecting the precipitation concentration among seven associated circulation indices in the Pearl River basin, and Huang et al. (2019) also explored the link between precipitation concentration and some monsoon indices in China. Several studies have investigated and revealed the spatio-temporal characters and the patterns of precipitation and flood/drought hazards in the HRB (Wang et al., 2016; He et al., 2015). Shi et al. (2014) examined the temporal features of precipitation concentration at the daily and monthly scales and held that most stations exhibited positive trends for the PCI and the CI, while none of the trends were significant at the 0.05 level for the PCI in the Huai River basin. However, detailed spatio-temporal behaviors of precipitation concentration still need to be further explored and the reasons for the changes of precipitation concentration have not been investigated in the HRB.

The structure of precipitation will have direct influences on the concentration characteristics of precipitation. For instance, total rainfall, rainy days, rainless days, continuous rainy days and continuous rainless days, rainfall of different grades and extreme precipitation, will all exert influences to a certain extent on the precipitation concentration. However, the relationship between the characteristics of precipitation concentration and the structure of precipitation has not been well understood so far. What is the relationship between the precipitation structure and the precipitation concentration? How do the changes of precipitation structure influence the precipitation concentration? This study firstly explored the spatio-temporal characteristics of the precipitation concentration in the HRB based on the Gini coefficient and further investigated comprehensively the relationship of the precipitation concentration with the structure of the precipitation by means of a set of precipitation indices, which can provide some indications for the mechanism of how precipitation concentration changes over the recent years in the study area. The study methods and research procedures demonstrated in this paper can provide useful reference for related study in other regions.

2. Methods and materials

2.1. Data

The data used in this study is derived from the precipitation observation data set provided by the National Meteorological Information Center, China. The National Meteorological Information Center has carried out strict quality control of the data, such as correcting some suspicious/false observations, and removing the heterogeneity caused by site migration and observation equipment upgrades. The data is the daily precipitation of 28 evenly distributed stations in the HRB from 1960 to 2014. All the 28 stations are national weather stations of China. All of them have the long term daily precipitation data with no missing data except for Heze and Linyi. Heze Station lacks the data during the periods from 1995 to 2006 and from 2009 to 2014; Linyi Station lacks the data during the periods from 1998 to 2006 and from 2009 to 2014. The location of the selected stations is shown in Fig. 1.

2.2. Methods

2.2.1. Precipitation concentration

Among the many precipitation concentration indices, Monjo and Martin-Vide (2016) recommended using the Gini coefficient due to its simplest estimation and its highest correlation ($R > 0.7$) with the other indices. The Gini coefficient is used to characterize the precipitation concentration in this study. The Gini coefficient measures the
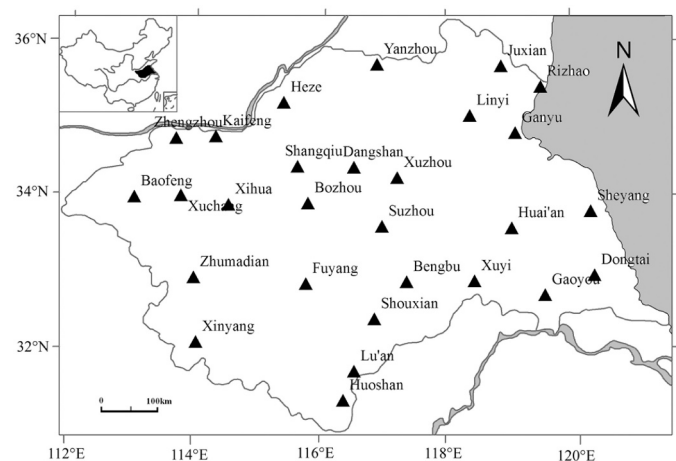

Fig. 1. Location of the Huai River basin (HRB) in China and distribution of the meteorological stations.

irregularity of the rainfall's temporal distribution by assessing the fraction of the rain contributed by the days belonging to each rainfall class (Martin-Vide, 2004; Burgueño et al., 2005). When an exponential distribution is fitted instead of the polygonal shape of the Lorenz curve, the resulting form of the Gini coefficient is named the concentration index (CI) (Martin-Vide, 2004).

In order to calculate the Gini coefficient, daily precipitation is reordered in ascending order, accumulated, and transformed into a fraction of the total precipitation, thus turning into a Lorenz curve (Yin et al., 2016). The Gini coefficient is then obtained by doubling the area within the Lorenz curve and the 45° diagonal line (which indicates that the precipitation follows a uniform distribution), which can be expressed as follows (Rajah et al., 2014):

$$Gini = \frac{1}{n}\left(n+1-2\left(\frac{\sum_{i=1}^{n}(n+1-i)y_i}{\sum_{i=1}^{n}y_i}\right)\right) \tag{1}$$

Where Gini stands for the Gini coefficient, y_i ($i = 1$ to n, n is the number of rainy days in the year, $y_i \leq y_i + 1$) stands for the precipitation of rainy days in a year.

2.2.2. Precipitation structure

The structure of precipitation can be represented by many precipitation indices such as total rainfall, rainy days, rainless days, continuous rainy days and rainless days, rainfall intensity, rainfall of different grades and extreme precipitation. The European Commission-funded project of Statistical and Regional Dynamical Downscaling of Extremes for European Regions (STARDEX) put forward 33 precipitation indices stem from the daily precipitation observation data (Haylock and Goodess, 2004; Moberg and Jones, 2005). A set of precipitation indices from STARDEX is selected to represent the structure of the precipitation in this study, which are listed in Table 1(AR, RD and PX1D are not included in the original 33 indices, which are added by the author). They are calculated by using the STARDEX Software in FORTRAN (available at http://www.cru.uea.ac.uk/cru/projects/stardex/).

In the selected indices, PQ20/PF20 can represent light rainfall, PQ40/PF40 and PQ50/PF50 can represent moderate rainfall, PQ80/PF80 can represent heavy rainfall, and PQ90/PF90, PQ95/PF95 can represent very heavy (or extreme) rainfall. PPWW (PPDD) refers to the proportion of continuous wet (dry) days to the total wet (dry) days, or the average persistence of wet (dry) days. PWSAV (PDSAV) refers to the average duration of wet (dry) days. PX1D、PX3D、PX5D and PX10D represent single-day and multi-day extreme precipitation. PNL90 and PFL90 refer to extreme precipitation events. AR refers to the annual rainfall, and RD refers to the annual number of rainy days. PINT is a simple daily intensity index, refers to the average rainfall amount of rainy days in the year, which is the ratio of AR to RD.

2.2.3. Composite analysis of the Gini

Composite analysis was utilized to explore the influences of flood and drought background on the Gini in the HRB. Typical flood and drought years were firstly selected based on the annual area rainfall in the basin. The composite mean and standard deviation (SD) of the Gini coefficients are the average of them during the typical flood and drought years. In order to determine the differences of the Gini between the flood/drought years and the long term average, the significance level of the composite mean and SD is examined by *t*-test, which is given by:

$$t = \frac{\overline{x} - \mu_0}{s}\sqrt{n} \tag{2}$$

Where $\overline{x}$ and s stand for the mean and standard deviation of typical flood/drought years respectively, μ_0 stands for the long-term average of the total series, and n refers to the number of typical (flood or drought) years.

3. Results and analysis

3.1. Spatio-temporal patterns of the Gini

3.1.1. Trend of the Gini

Fig. 2 shows the trend of the Gini coefficient of each station in the HRB. The majority of the stations exhibit no significant trend. However, there are more stations with positive trends than those with negative ones. Most of the stations have positive MK Z values and only three stations have negative Z values. However, only three of the stations with positive trend have passed the 0.05 significance level. Thus there is weak positive trend for the precipitation concentration in the HRB, indicating a slight tendency toward a more irregular precipitation distribution. Shi et al. (2014) also found upward trends in the precipitation concentration indices of the PCI and CI at most of the stations in the HRB during the period 1951 to 2010, while none of the trends were significant in the PCI. In fact, the trend of the precipitation concentration is not significant no matter it is increasing or decreasing in most of the previous studies (Yesilirmak and Atatanir, 2016; Sanguesa et al., 2018; Huang et al., 2018), with the study periods over 1966–2011, 1970–2016 and 1959–2015, respectively.

3.1.2. Spatial distribution of the Gini

In Fig. 3(a), the spatial distribution of the mean Gini coefficients shows a gradient of increase from the south to the north. On the one hand, the precipitation concentration is higher in the north than in the south; on the other hand, the precipitation is less in the north than in the south in the study area (the latter is well known due to the rainfall characteristics in China, so the figure is not shown), which indicates that the north part of the basin will face higher risk of severe drought. For the spatial distribution of the SD (standard deviation) of the Gini (Fig. 3(b)),
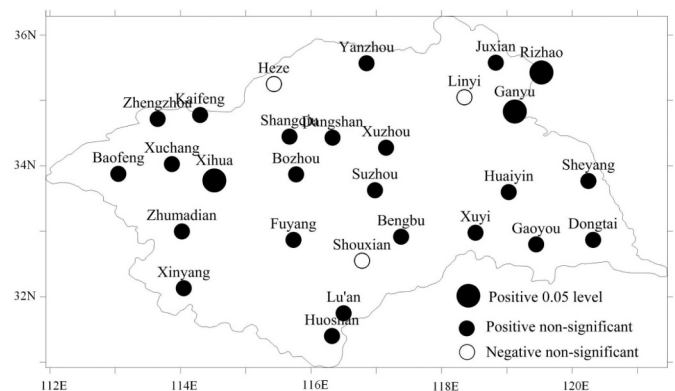
Table 1
The precipitation indices used to represent precipitation structure in this study.

Indices	Definition	Unit
PQ20/40/50/80/90/95	The 20th/40th/50th/80th/90th/95th percentile of rain-day amounts	mm
PF20/40/50/80/90/95	Fraction of total rainfall above annual 20th/40th/50th/80th/90th/95th percentile	%
PPWW/PPDD	Mean wet-day/dry-day persistence	-
PWSAV/PDSAV	Mean wet/dry spell lengths	day
PX1D/3D/5D/10D	Greatest 1-day/3-day/5-day/10-day total rainfall	mm
PNL90	Number of events bigger than the long-term 90th percentile	-
PFL90	Percent of total rainfall from events bigger than the long-term 90th percentile	%
AR	Annual rainfall	mm
RD	Rainy days	day
PINT	Simple Daily Intensity (rain per rainy day)	mm/day

Fig. 2. Mann-kendall trend of precipitation concentration characteristics of the Gini coefficient in the HRB from 1960 to 2014.
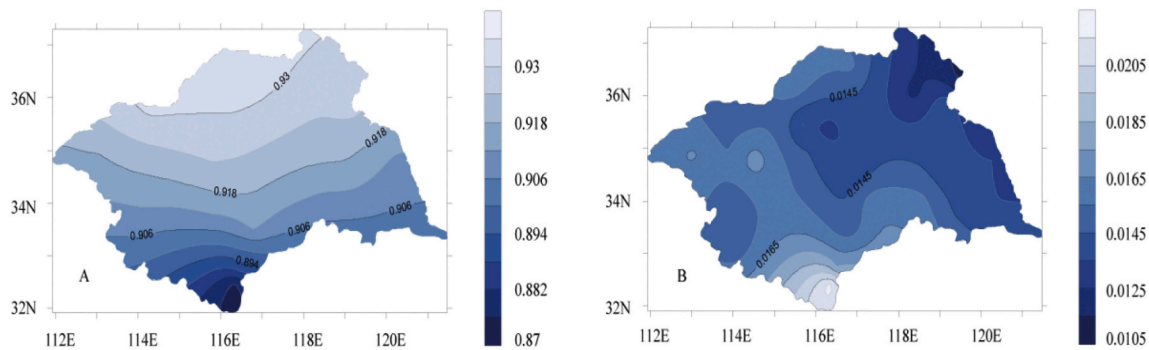
Fig. 3. Spatial distribution of of the mean (A) and standard deviation (B) of the Gini coefficient in the HRB from 1960 to 2014.

it is relatively low in the eastern (especially the northeastern) area but high in the western (especially the southwestern) areas, exhibiting a pattern decreasing from the southwest to the northeast. Thus the mean (stands for the central tendency) of the precipitation concentration increases with the increment of the latitude, while the SD (stands for the dispersion degree) of the precipitation concentration increases with the distances from the sea.

In the HRB, the mean of Gini is increasing from the south to the north, and the SD is increasing from the northeast to the southwest. However, according to Royéa and Martin-Videb (2017), the CI is high in the places where the latitude is low in the contiguous United States, and the CI and the CV (coefficient of variation, which is very similar to the SD) do not have statistically significant correlation. Sarricolea and Martin-Vide (2014) also found negative and significant correlation between the CI and the latitude in peninsular Spain. These are not consistent with our results. However, according to Sarricolea and Martin-Vide (2014), Benhamrouche et al. (2015), the correlation between the CI and the annual CV is positive and significant in Chile and Algeria. Therefore, the results of correlation analysis between them can vary from region to region.

3.1.3. EOF analysis of the Gini

EOF analysis obtained the spatiao-temporal pattern of the Gini coefficeints in the HRB (Fig. 4). The first three dominant modes pass the North test at the 0.05 significant level, and the fourth mode is at the 0.1 level. The EOF1 indicates a uniform pattern (explains 52.7% of the total variance),while the eigenevalues exhibit a pattern increasing from the east to the west parts. The EOF2 indicates a meridional dipole pattern (explains 10.6% of the total variance), while the eigenevalues exhibit a gradient increasing from the north to the south parts, with the highest vales locating in the southwestern end. The EOF3 implies a zonal dipole pattern (explains 6.9% of the total variance), with the eigenevalues increasing from the east to the west. And the EOF4 shows a tripole pattern of "+ − +" (only explains 3.8% of the total variance), with the eigenevalues increasing from the center to the north and the south. The southwest end of the study area has the highest eigenevalues of the Gini coefficient for all the four modes, indicating the strongest precipitation irregularity there. What's more, the spatial pattern of the mean and the SD of the Gini coefficient in Fig. 3 can both be found in the EOF modes in Fig. 4. The linear fitting curves of the corresponding principal components (PC1-PC4) of the first four modes show increasing trends except for PC2. Among them, only the increasing trend of PC4 passes the 0.1 significance level ($P = 0.063$). The weak upward trend of PC1 (i.e., the time coefficient of the leading mode) is consistent with the result of Fig. 2.

3.2. Composite Gini during typical years

This section examines the differences of the Gini during the typical flood and drought years. According to the annual area rainfall during

1960–2014 in the HRB, the ten years with the highest (lowest) annual area rainfall are defined as the typical flood (drought) years. The selected typical flood years are 1963, 1964, 1974, 1984, 1991, 1998, 2000, 2003, 2005 and 2007, and the typical drought years are 1966, 1976, 1978, 1981, 1986, 1988, 1997, 1999, 2001 and 2013.

Fig. 5 represents the composite mean and SD of the Gini coefficients in the flood and drought years. It is noted that the composite mean of the Gini coefficients in the drought years is larger than that in the flood years for all the stations, which is similar to the fact that the Gini in the north is higher than that in the south in Fig. 3 (Note that rainfall is higher in the south than in the north in the HRB). Generally, the composite mean of Gini coefficients is the biggest in the drought years (0.927 on average for the 28 stations), followed by the normal years (0.917 on average), and that in the flood years is the smallest (0.909 on average), i. e., the precipitation will be more concentrated when the year is drier. Therefore, it is more likely to cause the uneven distribution of the precipitation during the drought years when precipitation is low, which can aggravate the drought disasters. The significance test of the differences in the mean between typical flood and drought years showed that the *t* values of the 0.05 significance level with the degree of freedom of 18 are 2.1 and − 2.1. The results indicated that most of the stations (22 of them) reached the significance level of 0.05.

The composite SD of the Gini coefficients in the flood years is larger than that in the drought years for most of the stations. Generally, the SD in the flood years is the largest (0.016 on average for the 28 stations), followed by the normal years (0.015 on average), and that in the drought years is the smallest (0.011 on average). The Gini coefficient in the flood years is dispersed to a large extent, which indicates that the concentration is relatively small in certain years, but it can be very large in some other years. Therefore, the dispersion character of Gini coefficient will aggravate the flood disasters in certain years while it can also mitigate the flood disasters in some other years. For the significant test of the differences in the variance (i.e., the square of the SD) of the Gini coefficient between the typical flood and drought years, the *F* values at the 0.1 significance level for the degree of freedom (9, 9) are 3.18 and 0.31. The *F* values at the 0.05 significance level are 4.01 and 0.25. Results indicated that 8 stations passed the 0.1 significance level, and 4 stations passed the 0.05 significance level.

3.3. Relationship with precipitation structure changes

3.3.1. Relationship with AR and RD

Fig. 6 represents the annual series of AR, RD, PINT and the Gini over the HRB (the average of the 28 stations), their linear trends and decadal averages. Here, PINT is actually the ratio of AR to RD. There is a weak linear downward trend (not significant) in AR and there is a significant downward trend in RD. There is a significant upward trend in PINT while there is a weak upward trend (not significant) in the Gini. Besides, the decadal averages of AR/RD and those of the Gini are almost opposite: the former two almost continued to decrease (with only exceptions
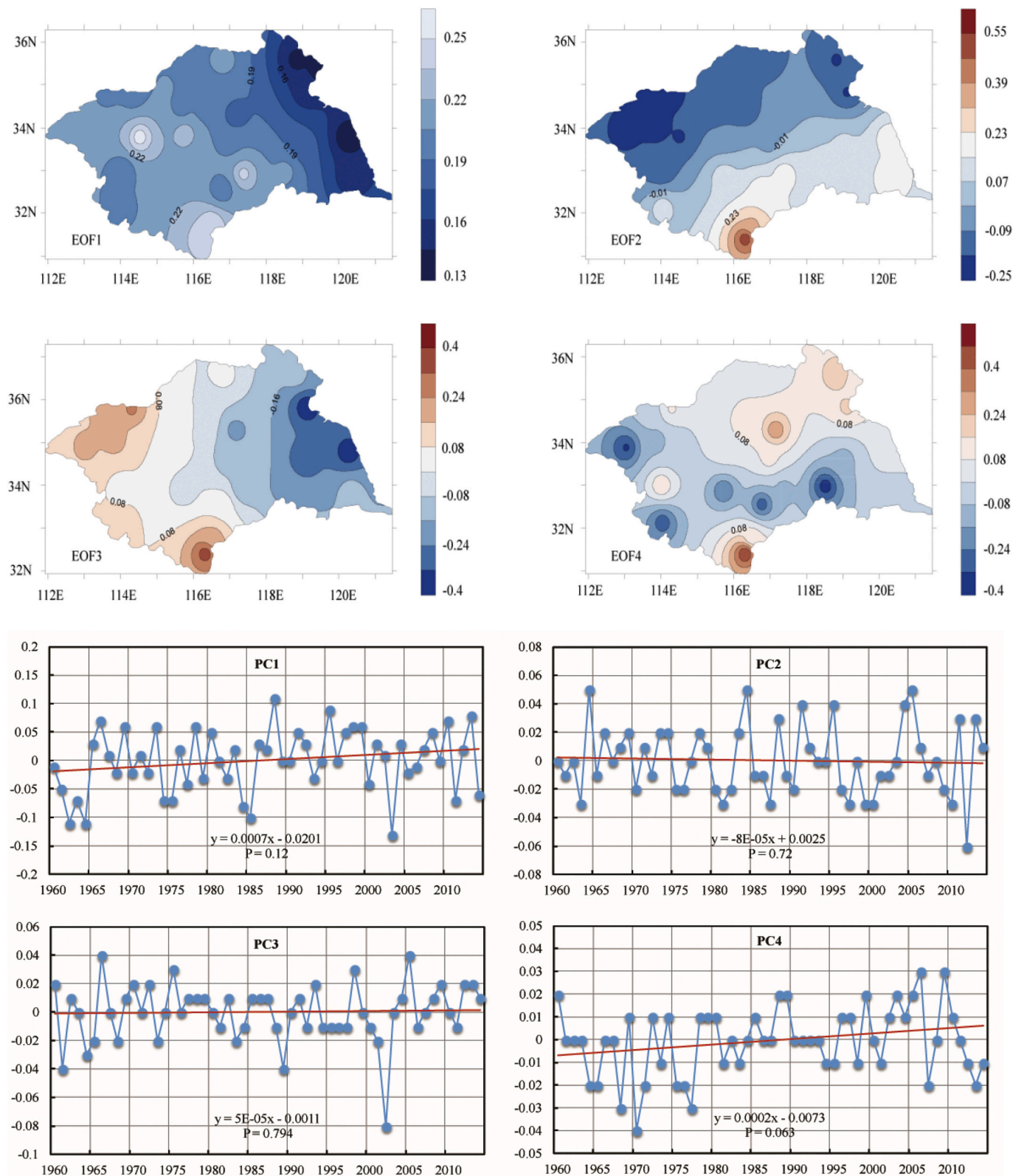
Fig. 4. Results of EOF analysis of concentration characteristics of the Gini coefficient in the HRB.

in the 2000s) and the latter almost continued to increase (with only exceptions in the 2000s and 2010s) from the 1960s to the 2010s. And the changes of decadal averages of PINT and those of the Gini are generally consistent (with only exceptions in the 2000s).

The correlation coefficients between the Gini and AR/RD/PINT station by station are shown in Fig. 7. Most of the stations are negatively correlated with an only exception in Fuyang Station for AR. All the stations are negatively correlated for RD while most of the stations are positively correlated with only two exceptions in Huaiyin and Rizhao for PINT. In addition, the correlation coefficients are significant at the 0.05
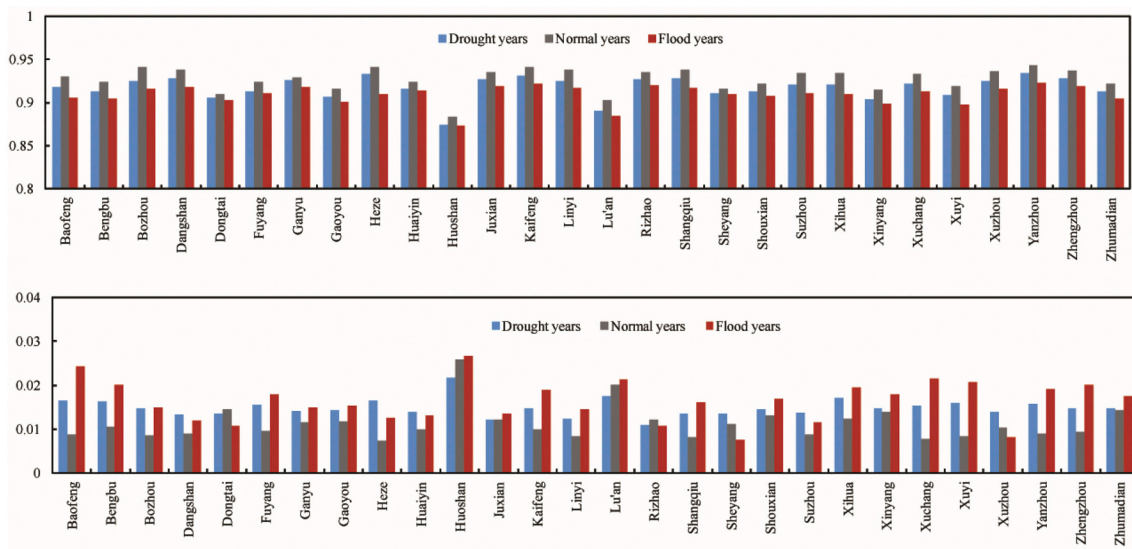
Fig. 5. Composite mean (A) and standard deviation (B) of the Gini coefficient in the typical flood and drought years.
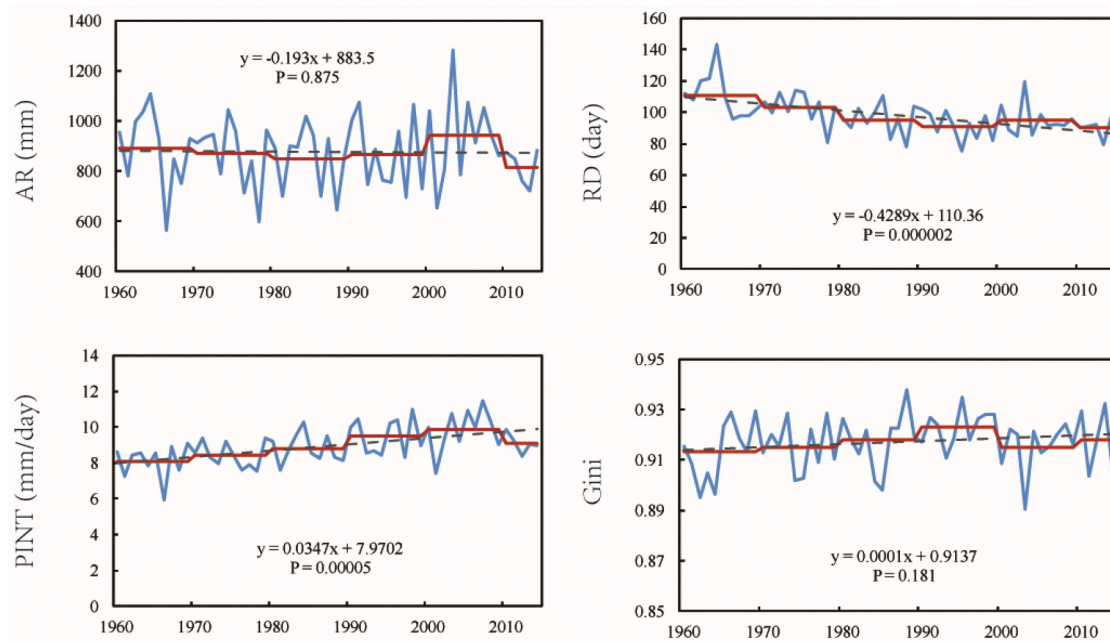

Fig. 6. The annual series of AR (a), RD (b), PINT (c) and the Gini coefficient (d) in the HRB from 1960 to 2014. (The dashed lines are the linear trends and the red lines indicate the decadal averages.)

level in all the stations for RD, in over half of the stations for AR, but in only a few stations for PINT.

According to Martin-Vide (2004), the precipitation concentration will be large where the annual precipitation is low; there is negative and non-significant correlation between the CI indices and the annual precipitation, but there is negative and significant correlation between the CI and the number of rainy days. Besides, Li et al. (2011), Coscarelli and Caloiero (2012), Benhamrouche et al. (2015) all came to the conclusion that the CI will be high in the places where the annual total precipitation and the number of rainy days are low. However, the correlation between the precipitation concentration and the number of rainy days can vary from region to region. A recent research (Monjo and Martin-Vide, 2016) indicated that there are negative correlations between the rainy days and precipitation concentration in the regions with uneven rainfall, while there are positive correlations in the regions with regular rainfall

patterns. In this study, however, the Gini had a significant negative correlation with both AR and RD, which is also consistent with the result in Fig. 3(a), since AR and RD are both higher in the south than in the north. Moreover, PINT is a simple index to measure the average rainfall intensity, which may not directly reveal the degree of the precipitation concentration (their correlation is not significant for most of the stations).

3.3.2. Relationship with the STARDEX indices

Fig. 8 summarizes the Mann-kendall trend results of the PQ and PF indices of the 28 stations in the HRB from 1960 to 2014. It is noted that there are evident differences between the trends in Fig. 2 and those in Figs. 8 and 10. This is because the non-significant trends for both positive and negative values are marked as no trend in Fig. 8, but the non-significant upward and downward trends are both labeled out in Fig. 2.
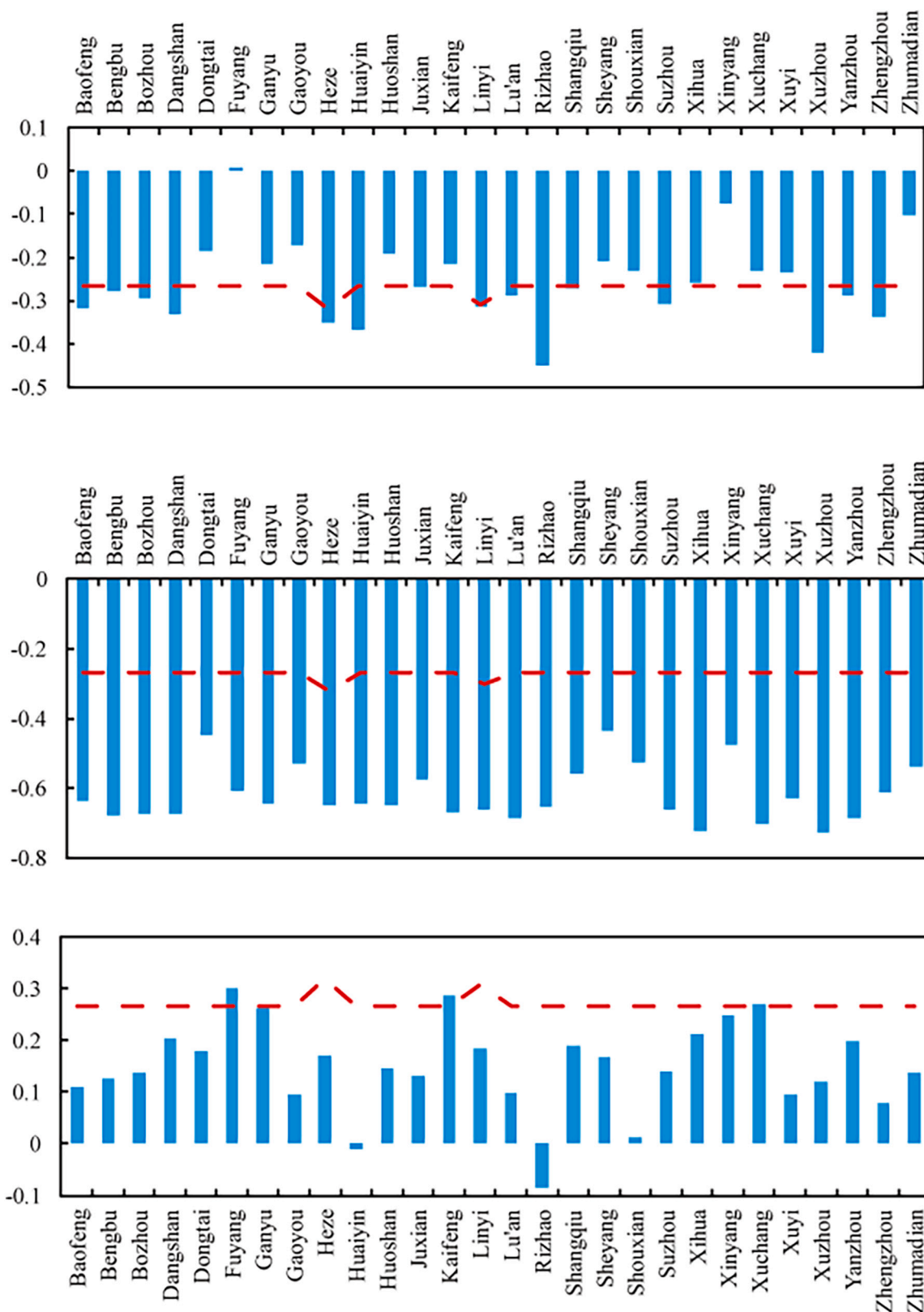
Fig. 7. Correlation coefficients between the Gini and AR/RD/PINT station by station in the HRB. Note: The dashed red lines indicate the 0.05 significant level.

Fig. 9 gives the box-plots of the annual indices (the average of the 28 stations) of PQ20 to PQ95 and PF20 to PF95 in the HRB. As can be seen, PQ20 is only about 1 mm; PQ40 is generally less than 3 mm; PQ50 is less than 5 mm; PQ80 is mainly between 10 and 20 mm; PQ90 is between 20 mm and 30 mm, and PQ95 is between 30 mm and 50 mm. PF95 is generally bigger than 30%, which indicates that the rainfall events greater than PQ95 generally account for more than 30% of the total rainfall. For PF90, the events greater than PQ90 generally reaches 50% of the total; and for PF80, the value is about 70%. Moreover, the average proportion of the rainfall larger than the median (i.e. PQ50) generally
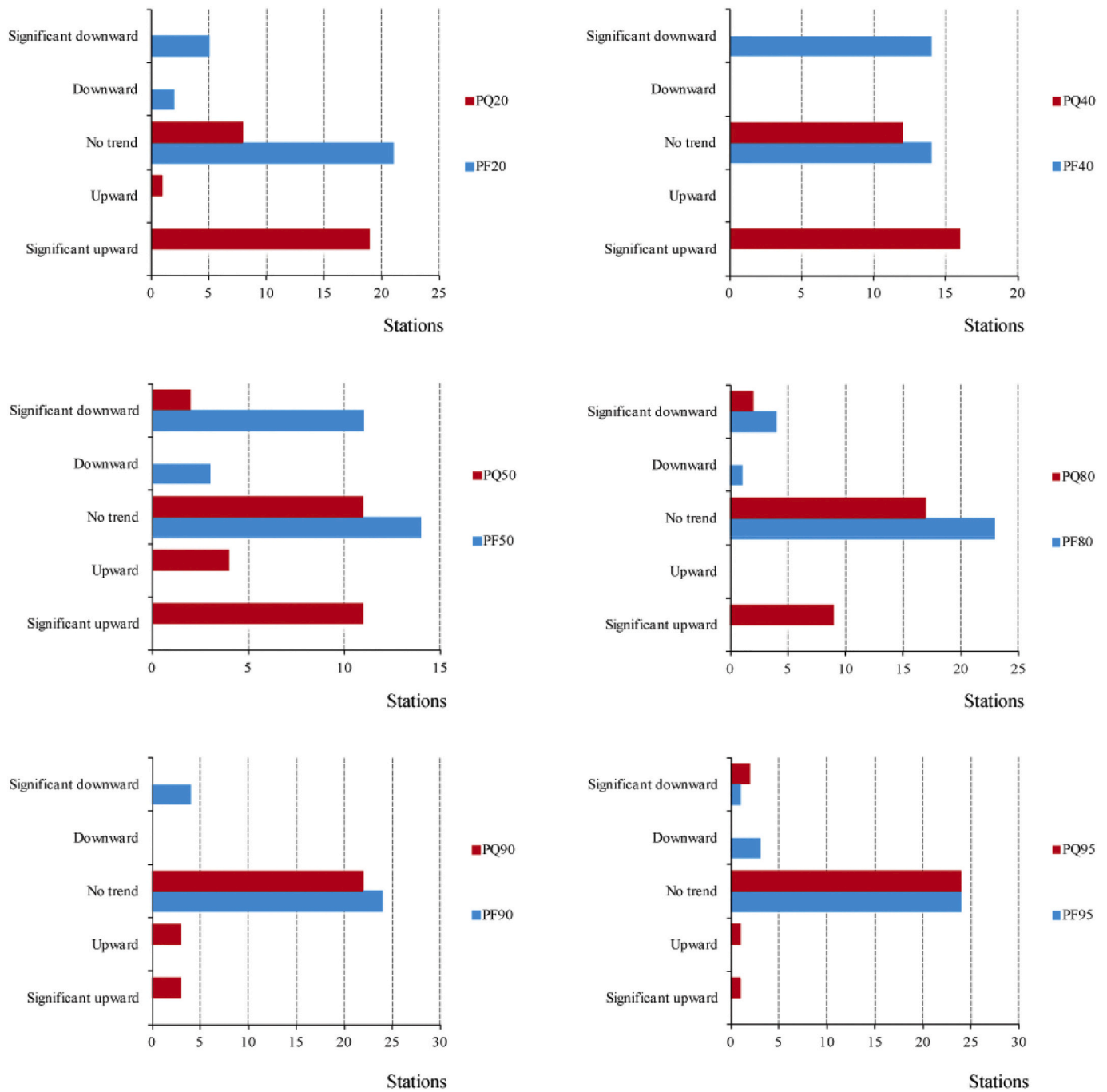
Fig. 8. Mann-kendall trends of the PQ and PF indices in the HRB from 1960 to 2014. (Significant upward and downward trends are at the 0.05 level, and upward and downward trends are at the 0.1 level.)

reaches 92% of the total, indicating that the rainfall events lower than PQ50 only accounts for about 8% of the total rainfall. And the results of PF40 and PF20 indicate that the events lower than PQ40 and PQ20 accounts for only about 4% and 2% of the total rainfall. Similarly, Zubieta et al. (2017) defined four categories (low, moderate, high and very high intensity) of rainfall based on percentiles, and the contributions of the four categories to the total rainfall are similar to our results according to their calculation.

It is found in Fig. 8 that, when we only consider the significant trend, the trend is mainly positive for the PQ indices from PQ20 to PQ95, while the trend is mainly negative for the PF indices from PF20 to PF95. The opposite trend is mainly due to the calculation method of the PF and PQ indices. The PF indices are the ratios which are bigger than the

corresponding thresholds, i.e., the PQ indices (which is sorted in ascending order), and thus the values of PQ and PF indices will be opposite in size. E.g., PF40/PF50 calculates the proportion of the rainfall over PQ40/PQ50, while PQ40/PQ50 refers to the 40/50th percentile of the rain-day amounts within a certain year, thus when the PQ40/50 values are high, the PF40/50 is low. And the trends of PF40/PF50 and PQ40/PQ50 tend to have opposite signs accordingly.

In Fig. 8, there are few stations where the trend of PQ80/PF80, PQ90/PF90 and PQ95/PF95 (i.e. heavy and very heavy rainfall) are significant, whether the trend is positive or negative. The only exception is PQ80: the number of stations with significant upward trend is up to 9, while most of the upward stations can be attributed to the contribution from winter, during which 7 stations have significant upward trend
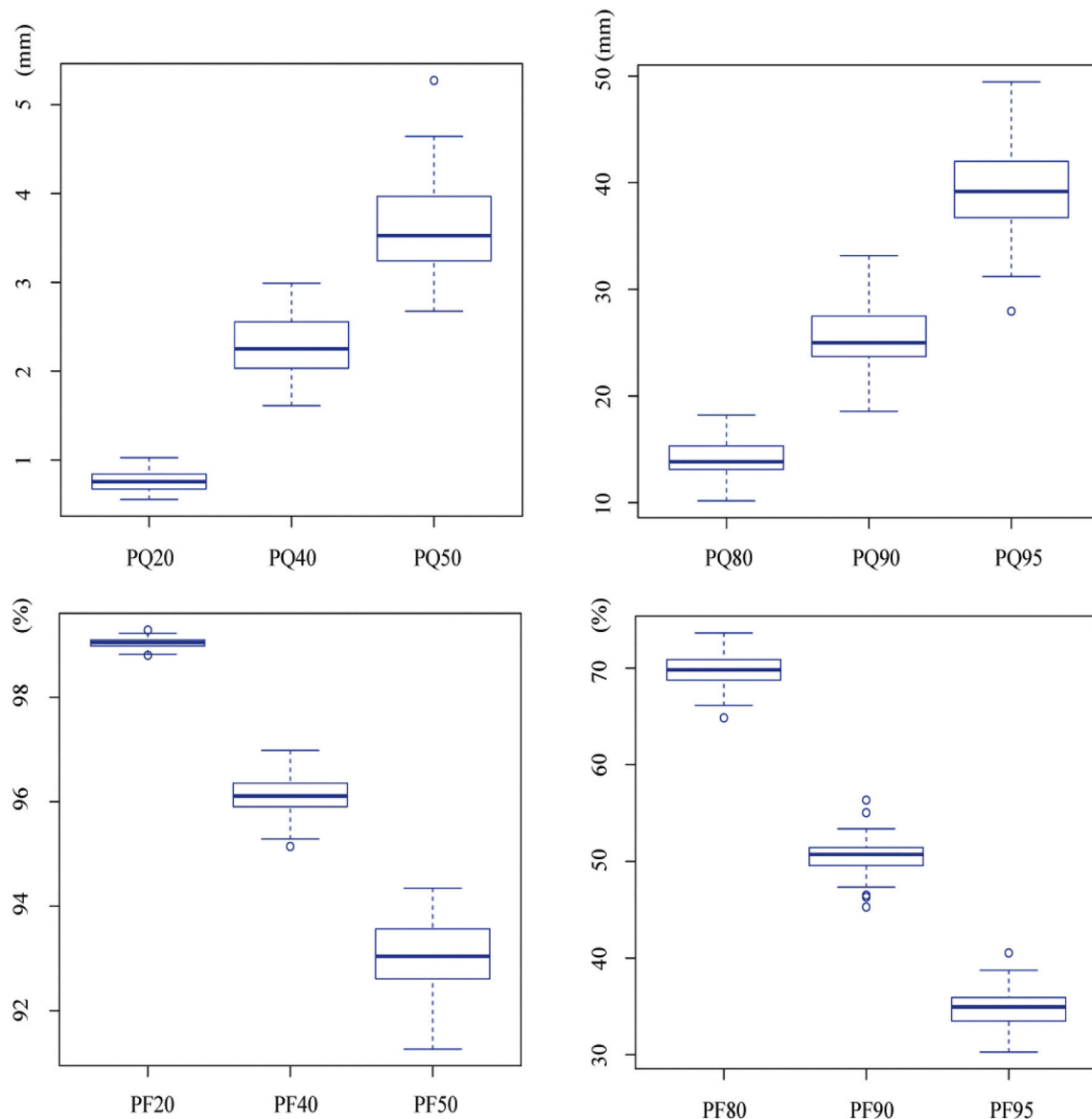
Fig. 9. Box-plots of annual average PQ indices (mm) and PF indices (%) in the HRB.

according to further analysis. PQ20, PQ40 and PQ50 have considerable stations (more than 10) with significant upward trend. Besides, PF20, PF40 and PF50 also have considerable stations (PF20 has 5 stations) with significant downward trend. The light and moderate rainfall of PQ20, PQ40 and PQ50 (corresponding PF20, PF40 and PF50) increased (decreased) quite significantly. Therefore, the weak upward trend of the Gini may mainly be associated with the upward trend of the light and moderate rainfall, not with that of the heavy or very heavy rainfall, and this may also be one of the reasons why the trend of the Gini is not significant.

Fig. 10 exhibits the trend of some other STARDEX indices. It is found that most of the stations have no trend in AR, and most of the stations have significant downward trend in RD (this is consistent with the results in Fig. 6). Neither PNL90 nor PFL90 has significant trend during the study period, and nor do the PX1D-PX10D indices. PPDD and PDSAV have significant upward trend in more than half of the stations while the downward trend of PPWW and PWSAV are generally not significant. The trends of the dry-day indices and wet-day indices are not exactly the opposite, and this may be because they are based on continuous dry and wet days, not the simple (scattered) dry and wet days.

Fig. 11 further represents the relationship between the Gini

coefficient and several typical STARDEX indices for all the 28 stations during 1960–2014 in the HRB (Each point represents the annual Gini and the corresponding precipitation indices of a station). As can be seen, PF95 and the Gini are significantly correlated with positive correlation coefficient, since the decision coefficient of the fitting line is high ($R^2 =$ 0.2055). This is also true for PF40. In general, the PF indices and the Gini are closely correlated, and the decision coefficients increase with the percentile increasing from 20 to 95 (i.e., from PF20 to PF95). However, the PQ indices are not significantly correlated with the Gini (decision coefficient is only 0.03 for PQ95). Firstly, the decision coefficients do not increase with the percentile increasing from 20 to 95. Secondly, both positive and negative correlation can occur for different percentiles (see the results of PQ95 and PQ40). The decision coefficient for PQ40 is also relatively high (nearly the same as that of PF40), but this is only an exception. The wet-day and dry-day indices of PWSAV and PDSAV have significant negative and positive correlation with the Gini, respectively (PPWW and PPDD are the same, not shown here).

Besides, AR and RD are significantly correlated with the Gini (both negatively) but PINT is not, which is consistent with the results in Fig. 7. And the relationship between the extreme precipitation indices of PX1D-PX10D, PNL90, PFL90 and the Gini is not significant. The results of these
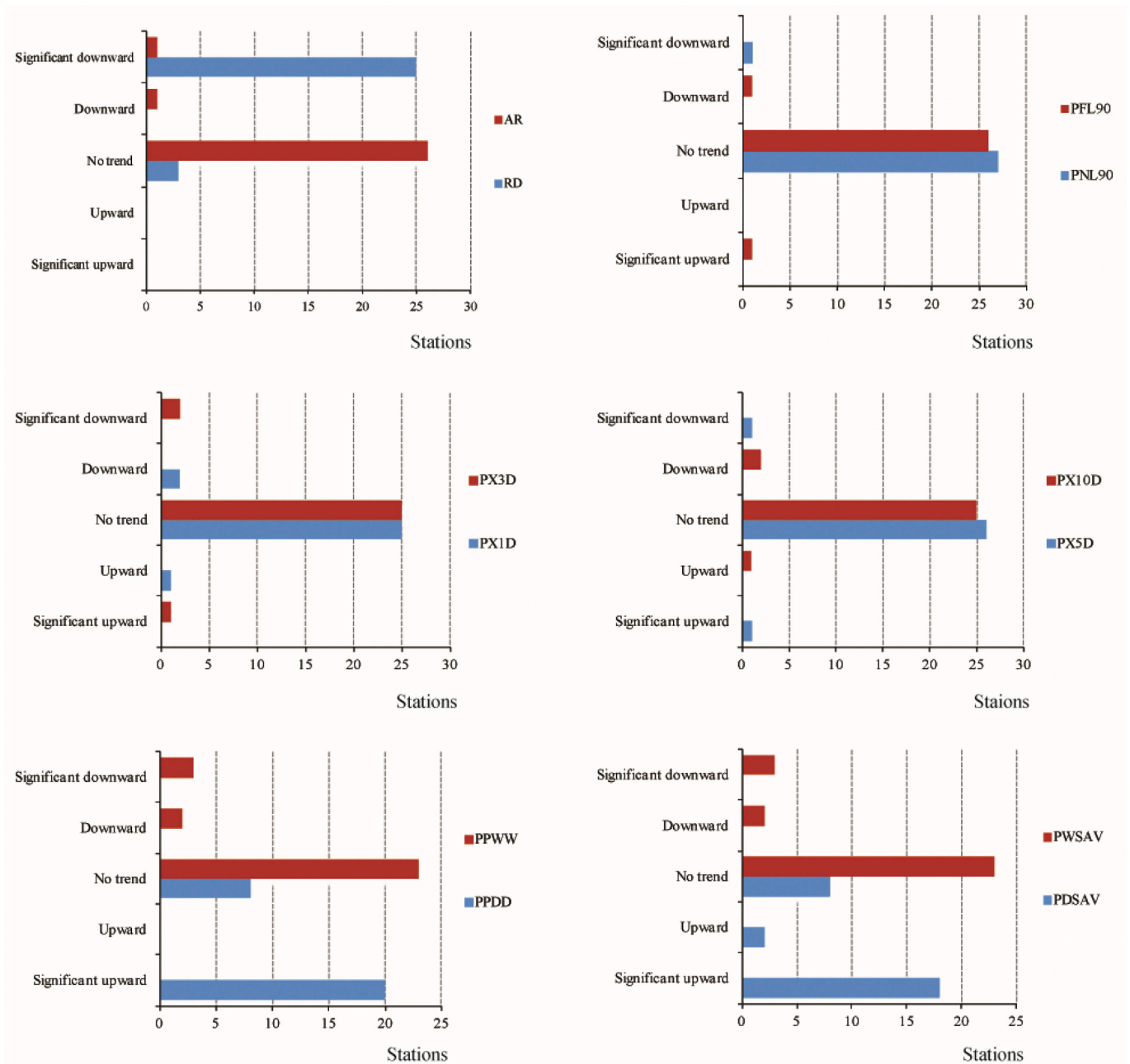
Fig. 10. Mann-kendall trends of precipitation indices of rainfall (AR and RD), wet-day and dry-day indices (PWSAV, PDSAV, PPWW, PPDD) and extreme precipitation (PX1D-PX10D, PNL90, PFL90) in the HRB from 1960 to 2014. (Significant upward and downward trends are at the 0.05 level, and upward and downward trends are at the 0.1 level.)

indices are not shown.

3.4. Discussions

The relationship between the precipitation concentration and the precipitation structure represented by a set of precipitation indices is explored in this study. The light and moderate rainfall (PF/PQ20, PF/ PQ40, PF/PQ50) increased significantly in a lot of stations, and the heavy and very heavy rainfall increased significantly in only a few stations. However, there is a significant upward trend in PINT (the simple daily rainfall intensity), thus the increase of PINT is mainly due to the increment of light and moderate rainfall. And the non-significant increase of the Gini is also linked to the increment of light and moderate rainfall according to the above analysis in section 3.3.2. The decrease of

the wet-day indices of PPWW and PWSAV (refer to continuous wet days) is not significant, but the decrease of the RD is significant, i.e., the simple, scattered rainy days decreased significantly. But the continuous wet days can better reflect the precipitation concentration than the simple, scattered wet days. Therefore, when we are analyzing the relationship between rainy days and the precipitation concentration, it is better to consider the continuous rainy days, ie. the indices of PPWW and PWSAV.

The Gini is not significantly correlated with the extreme precipitation (PX1D-PX10D, PNL90 and PFL90), and there is also no significant trend in extreme precipitation. And the Gini is significantly correlated with the PF indices, but not for the PQ indices. Besides, the Gini is also not significantly correlated with the PINT.

To sum up, the non-significant increase of the Gini coefficient in the
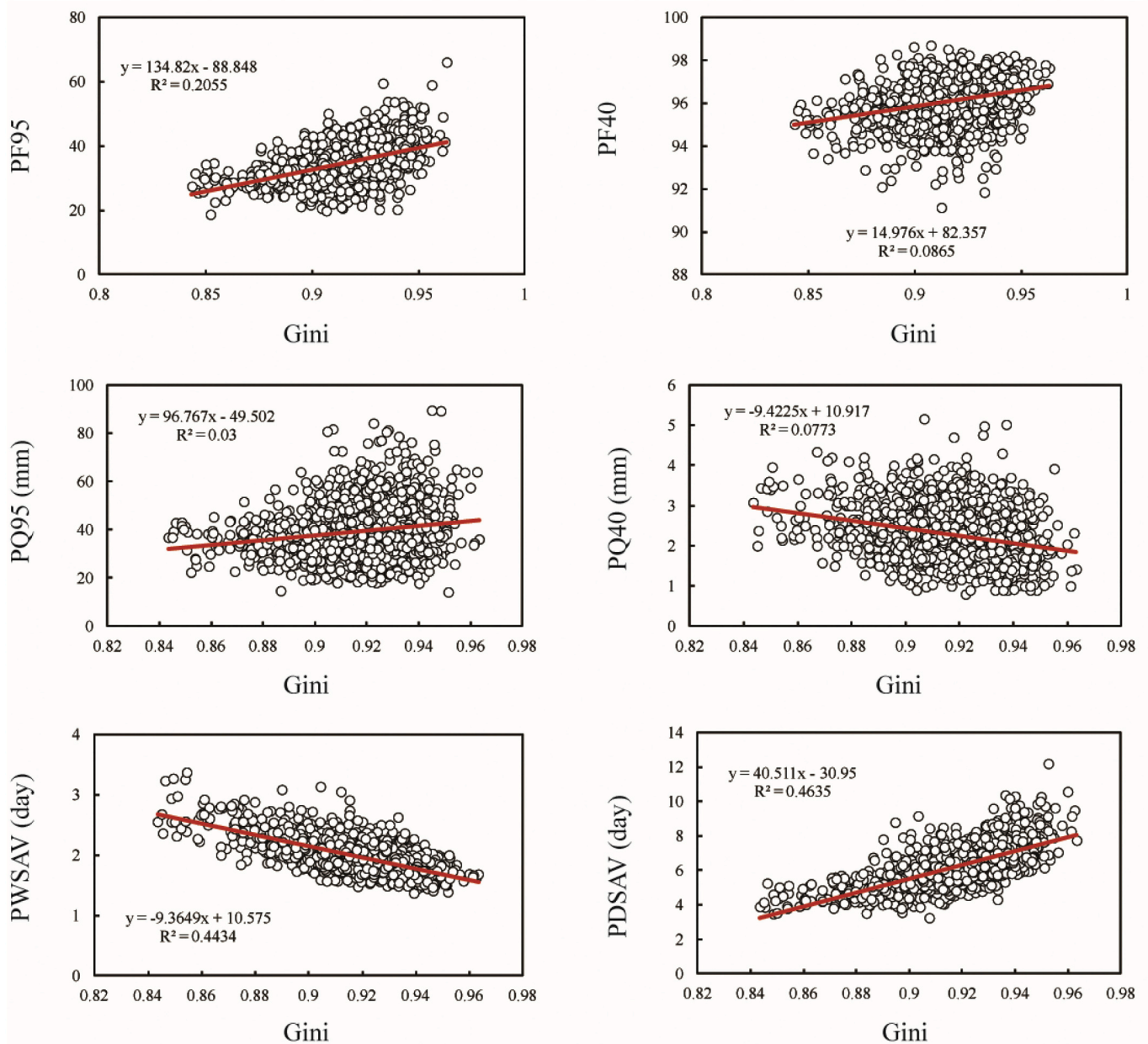
Fig. 11. Relationship between the Gini coefficient and several typical STARDEX indices for all the 28 stations during 1960–2014 in the HRB.

study area is caused neither by the heavy and extreme precipitation, nor by the PQ indices. But the increase of the Gini coefficient is mainly associated with AR, RD, the light and moderate rainfall (mainly PF20, PF40, PF50) and the wet-day and dry-day indices (PPWW, PWSAV, PPDD and PDSAV).

4. Conclusions

This study explored the concentration characteristics of the precipitation in the Huai River basin based on the Gini coefficient and investigated the relationship between the precipitation concentration and the structure of precipitation by means of a set of precipitation indices, and the following conclusions can be obtained:

(1) There is a non-significant upward trend for the precipitation concentration (the Gini) in the HRB. The mean of the Gini shows a spatial pattern of increase from the south to the north, and the SD

of the Gini shows a pattern of increase from the northeast to the southwest.

(2) The first mode of EOF analysis indicates a uniform pattern, the second mode indicates a meridional dipole pattern, the third mode implies a zonal dipole pattern, and the fourth pattern shows a tripole pattern in the HRB.

(3) The composite mean of Gini coefficients in the drought years is larger than that in the flood years for all the stations, which can aggravate the drought disasters during the drought years when precipitation is low. The composite SD of Gini in the flood years is larger than that in the drought years for most of the stations.

(4) The non-significant increase of the Gini coefficient in the study area is caused neither by the heavy and extreme precipitation, nor by the PQ indices. But the increase of the Gini coefficient is mainly associated with AR, RD, the light and moderate rainfall (mainly PF20, PF40, PF50) and the wet-day and dry-day indices.

Previous studies mainly focus on the spatial and temporal changes of

the precipitation concentration. However, in-depth research which probes into the reasons and mechanisms of the changes is not enough. This study is the first time to investigate in detail the reasons of the precipitation concentration changes based on the structure of the precipitation represented by a set of precipitation indices. Because the trend of the Gini is not significant in the study area, it is not easy to detect the relationship between the change of precipitation structure and the precipitation concentration. If the trend of the precipitation concentration is significant, it may be easier to find the relationship between them. Besides, the related mechanisms based on atmospheric circulation needs further exploration in the future.

Declaration of Competing Interest

The authors declare no conflict of interest.

Acknowledgments

References

Benhamrouche, A., Boucherf, D., Hamadache, R., et al., 2015. Spatial distribution of the daily precipitation concentration index in Algeria. Nat. Hazards Earth Syst. Sci. 15, 617–625.

Burgueño, A., Martínez, M.D., Lana, X., et al., 2005. Statistical distributions of the daily rainfall regime in Catalonia (Northeastern Spain) for the years 1950–2000. Int. J. Climatol. 25, 1381–1403.

Coscarelli, R., Caloiero, T., 2012. Analysis of daily and monthly rainfall concentration in Southern Italy(Calabria region). J. Hydrol. 416–417, 145–156.

Dai, A.G., 2013. Increasing drought under global warming in observations and models. Nat. Clim. Change 3 (1), 52–58.

Groisman, P.Y., Knight, R.W., Easterling, D.R., et al., 2005. Trends in intense precipitation in the climate record. J. Clim. 18 (9), 1326–1350.

Guo, E.L., Wang, Y.F., Jirigala, B., et al., 2020. Spatiotemporal variations of precipitation concentration and their potential links to drought in mainland China. J. Clean. Prod. 267, 122004.

Haylock, M.R., Goodess, C.M., 2004. Interannual variability of European extreme winter rainfall and links with mean large-scale circulation. Int. J. Climatol. 24 (6), 759–776.

He, Y., Ye, J., Yang, X., 2015. Analysis of the spatio-temporal patterns of dry and wet conditions in the Huai River Basin using the standardized precipitation index. Atmos. Res. 166, 120–128.

Huang, Y., Wang, H., Xiao, W.H., et al., 2018. Spatial and temporal variability in the precipitation concentration in the upper reaches of the Hongshui River Basin, Southwestern China. Adv. Meteorol. 2018, 1–19.

Huang, Y., Wang, H., Xiao, W.H., et al., 2019. Spatiotemporal characteristics of precipitation concentration and the possible links of precipitation to monsoons in China from 1960 to 2015. Theor. Appl. Climatol. 138, 135–152.

Jiang, P., Wang, D.G., Cao, Y.Q., 2016. Spatiotemporal characteristics of precipitation concentration and their possible links to urban extent in China. Theor. Appl. Climatol. 123 (3–4), 757–768.

Jongman, B., Ward, P.J., Aerts, J.C.J.H., 2012. Global exposure to river and coastal flooding: long term trends and changes. Glob. Environ. Chang. 22, 823–835.

Li, X.M., Jiang, F.Q., Li, L.H., et al., 2011. Spatial and temporal variability of precipitation concentration index, concentration degree and concentration period in Xinjiang, China. Int. J. Climatol. 31, 1679–1693.

Li, H., Zhai, P.M., Lu, E., et al., 2017. Changes in temporal concentration property of summer precipitation in China during 1961–2010 based on a new index. J. Meteorol. Res. 31 (2), 336–349.

Llano, M.P., 2018. Spatial distribution of the daily rainfall concentration index in Argentina: comparison with other countries. Theor. Appl. Climatol. 133 (3–4), 997–1007.

Martin-Vide, J., 2004. Spatial distribution of a daily precipitation concentration index in peninsular Spain. Int. J. Climatol. 24, 959–971.

Moberg, A., Jones, P.D., 2005. Trends in indices for extremes in daily temperature and precipitation in central and western Europe, 1901-99. Int. J. Climatol. 25 (9), 1149–1171.

Monjo, R., Martin-Vide, J., 2016. Daily precipitation concentration around the world according to several indices. Int. J. Climatol. 36 (11), 3828–3838.

Nery, J.T., Carfan, A.C., Martin-Vide, J., 2017. Analysis of rain variability using the daily and monthly concentration indexes in Southeastern Brazil. Atmos. Clim. Sci. 7 (2), 176–190.

Oliver, J.E., 1980. Monthly precipitation distribution: a comparative index. Prof. Geogr. 32, 300.

Rahman, M.S., Islam, A.R.M.T., 2019. Are precipitation concentration and intensity changing in Bangladesh overtimes? Analysis of the possible causes of changes in precipitation systems. Sci. Total Environ. 690, 370–387.

Rajah, K., O'Leary, T., Turner, A., et al., 2014. Changes to the temporal distribution of daily precipitation. Geophys. Res. Lett. 41 (24), 8887–8894.

Royéa, D., Martin-Videb, J., 2017. Concentration of daily precipitation in the contiguous United States. Atmos. Res. 196, 237–247.

Sanguesa, C., Pizarro, R., Ibanez, A., et al., 2018. Spatial and temporal analysis of rainfall concentration using the Gini index and PCI. Water 10 (2), 112. https://doi.org/10.3390/w10020112.

Sarricolea, P., Martin-Vide, J., 2014. Spatial analysis of rainfall daily trends and concentration in Chile. Investig. Geogr. Chile 47, 53–66.

Sarricolea, P., Meseguer-Ruiz, O., Serrano-Notivoli, R., et al., 2019. Trends of daily precipitation concentration in Central-Southern Chile. Atmos. Res. 215, 85–98.

Serrano-Notivoli, R., Martín-Vide, J., Saz, M.A., et al., 2018. Spatio-temporal variability of daily precipitation concentration in Spain based on a high-resolution gridded data set. Int. J. Climatol. 38 (S1), e518–e530.

Shi, P., Qiao, X.Y., Chen, X., et al., 2014. Spatial distribution and temporal trends in daily and monthly precipitation concentration indices in the upper reaches of the Huai River, China. Stoch. Env. Res. Risk A. 28 (2), 201–212.

Simpson, I.R., Jones, P.D., 2014. Analysis of UK precipitation extremes derived from Met Office gridded data. Int. J. Climatol. 34 (7), 2438–2449.

Visser, H., Petersen, A.C., Ligtvoet, W., 2014. On the relation between weather-related disaster impacts, vulnerability and climate change. Clim. Chang. 125, 461–477.

Wang, Y., Zhang, Q., Singh, V.P., 2016. Spatiotemporal patterns of precipitation regimes in the Huai River basin, China, and possible relations with ENSO events. Nat. Hazards 82 (3), 2167–2185.

Yang, P., Zhang, Y.Y., Xia, J., et al., 2020. Investigation of precipitation concentration and trends and their potential drivers in the major river basins of Central Asia. Atmos. Res. 245, 105128.

Yesilirmak, E., Atatanir, L., 2016. Spatiotemporal variability of precipitation concentration in western Turkey. Nat. Hazards 81 (1), 687–704.

Yin, Y.X., Xu, C.-Y., Chen, H.S., et al., 2016. Trend and concentration characteristics of precipitation and related climatic teleconnections from 1982 to 2010 in the Beas River basin, India. Glob. Planet. Chang. 145, 116–129.

Yin, Y.X., Chen, H.S., Zhai, P.M., et al., 2019. Characteristics of summer extreme precipitation in the Huai River basin and their relationship with East Asia summer monsoon during 1960 to 2014. Int. J. Climatol. 39 (3), 1555–1570.

Zhai, P.M., Zhang, X.B., Wan, H., et al., 2005. Trends in total precipitation and frequency of daily precipitation extremes over China. J. Clim. 18 (7), 1096–1108.

Zhang, L.J., Qian, Y.F., 2003. Annual distribution features of precipitation in China and their interannual variations. Acta Meteorol. Sin. 17, 146–163.

Zhang, Y.Y., Xia, J., Liang, T., et al., 2010. Impact of water projects on river flow regime and water quality in Huai River basin. Water Resour. Manag. 24, 889–908.

Zhao, C.S., Sun, C.L., Liu, C.M., et al., 2014. Analysis of regional zoobenthos status in the Huai River basin, China using two new ecological niche clustering approaches. Ecohydrology 7, 91–101.

Zheng, Y.H., He, Y.H., Chen, X.H., 2017. Spatiotemporal pattern of precipitation concentration and its possible causes in the Pearl River basin, China. J. Clean. Prod. 161, 1020–1031.

Zubieta, R., Saavedra, M., Silva, Y., et al., 2017. Spatial analysis and temporal trends of daily precipitation concentration in the Mantaro river basin: Central Andes of Peru. Stoch. Env. Res. Risk A. 31 (6), 1305–1318.